JOURNAL OF Materials CHEMISTRY

Hierarchically ordered networks comprising crystalline ZrO_2 tubes through sol–gel mineralization of eggshell membranes

Dong Yang, Limin Qi* and Jiming Ma

State Key Laboratory for Structural Chemistry of Stable and Unstable Species, College of Chemistry, Peking University, Beijing 100871, China. E-mail: liminqi@chem.pku.edu.cn

Received 28th January 2003, Accepted 20th March 2003
First published as an Advance Article on the web 28th March 2003

A facile sol–gel coating procedure has been successfully applied for the ZrO_2 coating of eggshell membranes (ESM), resulting in hierarchically ordered thin films with a macroporous network structure comprising crystalline ZrO_2 tubes. This hierarchical material, which was obtained through sol–gel mineralization of the ESM template and subsequent calcination at 600 °C, was characterized by XRD, SEM, TEM, HRTEM, and nitrogen sorption measurements. It has been shown that this ZrO_2 material exhibits a macroscopic morphology of a film with a thickness about 15 μm; the film has a microstructure of macroporous networks composed of interwoven ZrO_2 microtubes with diameters less than 1.0 μm; the tube walls consist of tetragonal ZrO_2 nanocrystals with an average crystallite size about 6 nm. It shows a specific surface area of 55 $m^2\ g^{-1}$ and a BET average pore size of 7.0 nm, which is mostly due to the ZrO_2 nanocrystals constituting the tube walls. It has also been shown that calcination of the initial ESM/zirconium precursor hybrid at 700 °C resulted in significant fusion between neighboring ZrO_2 tubes accompanying a tetragonal-to-monoclinic phase transformation of zirconia.

Introduction

Porous inorganic materials with controlled pore structure and size have attracted much attention because of their wide potential applications in catalysis, sorption, separation, and optics. In general, strategies for synthesizing these materials rely on the use of templates, the size and nature of which dictate the pore dimensions and architecture. For example, three-dimensional (3-D) ordered macroporus materials have been fabricated by using various templates including colloidal crystals,[1–4] polyurethane foams,[5] and emulsions[6] whereas ordered mesoporous materials have been synthesized by templating organized assemblies of surfactants[7] and block copolymers.[8,9] Macroporous networks have also been prepared by employing polymer gels,[10,11] polymer membranes,[12,13] and bicontinuous microemulsions[14,15] as templates. In addition to synthetic templates, a variety of natural biological templates have been employed for the synthesis of porous materials with sophisticated structural ordering analogous to natural materials.[16–22]

Compared with artificial templates, biological templates are inherently complex and hierarchical;[23,24] moreover, they are generally cheap, abundant, and environmentally benign. For instance, sophisticated macroporous materials have been produced by templating organic matrix isolated from cuttlebone[16] and inorganic skeletal plates of echinoids.[17] Notably, biological templates, such as organized bacterial threads[18,19] and wood cellular structures,[20,21] have been used to synthesize hierarchically ordered macroporous materials with bimodal porosity, which combined the good mass transport and accessibility of macroporous networks with the high surface area, selectivity, and catalytic properties of the smaller pore systems. Recently, we reported a novel synthesis of hierarchically ordered macroporous networks composed of TiO_2 tubes by using eggshell membranes (ESM) as templates *via* a sol–gel coating method.[22] However, this ESM templating approach remains to be extended to the synthesis of hierarchically ordered networks of other oxide systems.

Zirconium dioxide has attracted increasing interest in the field of heterogeneous catalysis since it has redox properties as well as acidic and basic character.[25] Its high chemical stability also favors its applications as a catalyst support, adsorbent, chemical sensor, and structural ceramic.[26,27] Consequently, the fabrication and structural characterization of ZrO_2 nanoparticles[27–29] and nanotubes[30,31] have attracted much attention. On the other hand, many recent efforts have been devoted to the synthesis of porous ZrO_2 with controlled pore structure and size; examples include ordered mesoporous ZrO_2,[9,26,32–34] ordered macroporous ZrO_2,[6,35] and high-surface-area ZrO_2 aerogels.[25] It is noteworthy that macroporous ZrO_2 network membranes have been easily fabricated by sol–gel coating[36] of cellulose acetate (CA) membranes.[12] However, in many cases the obtained porous ZrO_2 materials were not well-crystallized, which would largely limit their applications in catalysis. Furthermore, it would be highly desirable to synthesize hierarchically ordered porous ZrO_2 since the control of pore structure and size greatly influences the efficiency of the porous material in its applications. In this current work, we have applied the sol–gel coating procedure for the ZrO_2 coating of ESM consisting of interwoven organic fibers. For the first time, hierarchically ordered network membranes comprising crystalline ZrO_2 tubes have been prepared through the sol–gel mineralization of ESM.

Experimental

Materials

The zirconium precursor, zirconium propoxide (ZP, 70 wt% in propanol) was purchased from Fluka. Commercial eggs were locally available. All the other chemicals used in the experiments were of analytical grade and the water used was deionized.

Separation of eggshell membranes

Eggshell membranes (ESM), which are stable in aqueous and alcoholic media and undergo pyrolysis on heating, consist of the outer shell membrane, inner shell membrane, and limiting membrane surrounding the egg white.[37] The outer shell

membrane, which can be easily isolated from eggshells, was used as a removable template in this work. The separation of the outer shell membrane from eggs has been described previously.[22] Briefly, eggs were gently broken and emptied *via* the blunt end and the eggshells were washed with water. Then, the inner shell membrane and the limiting membrane were manually removed. The remaining eggshells were rinsed in 1 M HCl to dissolve the $CaCO_3$, leaving the organic outer shell membrane. After the outer shell membrane was washed with water thoroughly, a solvent exchange process for the membrane was carried out by slowly increasing the ratio of 2-propanol to water until the membrane was in high purity 2-propanol (99.7%), similar to the case of polymer gels.[12] Then the dehydrated outer shell membrane was used as the ESM template for the ZrO_2 coating.

Sol–gel mineralization of ZrO_2

The sol–gel coating procedure previously used for the TiO_2 coating of the ESM template[22] was partly modified and applied for the ZrO_2 coating. In a typical synthesis, the eggshell membrane was dipped into a closed vessel containing a 7% (w/w) solution of zirconium propoxide (ZP) in 2-propanol for 4 h, where an equimolar amount of acetyl acetone (acac) was added to lower the hydrolysis rate of ZP. After removal from this solution, the membrane coated with the precursor was dried in air at room temperature for 48 h. The resulting yellow hybrid material was then heated to 600 °C or 700 °C in an oven under air atmosphere to burn off the organics and crystallize zirconia.

It can be noted that for the synthesis of ESM-templated TiO_2, the ESM template filled with the precursor titanium butoxide (TB) was hydrolyzed in 2-propanol/water (50 : 50 v/v) for 1 h before it was dried in air.[22] However, our preliminary experiment showed that if the same procedure was applied for the synthesis of ESM-templated ZrO_2, lots of irregular ZrO_2 particles stuck on the surface of the membrane and the ESM template could not be replicated well, which could be attributed to the much faster hydrolysis rate of ZP. Consequently, ZP-coated ESM was directly dried in air without hydrolysis in the 2-propanol/water mixture in the present preparation. It was also found that if the dipping time of the ESM template in the ZP solution was shorter than 1 h, the precursor ZP did not form a complete coating on the surfaces of the ESM fibers, resulting in collapsed ZrO_2 membranes upon drying and calcination. When the dipping time was varied from 4 to 24 h, the ESM template could be replicated well and the structure of the resulting ZrO_2 material did not change considerably. Hence, a dipping time of 4 h was adopted in this work.

Characterization

Scanning electron microscopy (SEM) measurements were performed with an Amray 1910FE microscope. Transmission electron microscopy (TEM) and high-resolution transmission electron microscopy (HRTEM) investigations were conducted on a JEOL JEM-200CX microscope and a Hitachi H-9000HAR microscope, respectively. Powder X-ray diffraction (XRD) patterns were recorded on a Rigaku Dmax-2000 diffractometer with Cu Kα radiation. Themogravimetric analysis (TGA) was carried out on a LCT-1 type thermoanalyzer in air. The specific surface area and average pore size were obtained from BET analysis after nitrogen sorption using a Micromeritics ASAP 2010 system.

Results and discussion

It has been documented that avian eggshells are formed by layered organization of calcified shell and organic eggshell membranes consisting of collagen-like proteins (collagen types I, V, and X) and glycosaminoglycans.[38] Scanning electron microscopy (SEM) images present information about the membrane thickness and the larger pores in the initial membrane template. Typical SEM images of the initial ESM template are presented in Fig. 1. As shown in Fig. 1a, the membrane has a macroporous framework composed of interwoven and coalescing fibers ranging from 0.5 to 1.5 μm in diameter. A membrane thickness of about 25 μm can be estimated from the cross section image (Fig. 1b).

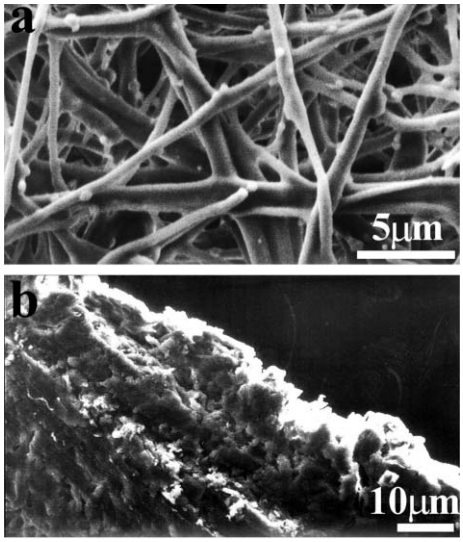

Fig. 1 SEM images of the eggshell membrane (ESM) template. (a) Overview of the surface of ESM, (b) overview of the cross section of ESM.

It is known that eggshell membranes contain plenty of amines, amides and carboxylic surface functional groups,[39] which may interact with the zirconium precursor, anchoring the precursor molecules to the membrane fiber surface where the ZP coating can occur. The TGA curve of the resulting ESM/ZP hybrid is shown in Fig. 2, which suggests that the organic ESM template and the zirconium precursor started pyrolyzing around 210 °C and were completely pyrolyzed by 600 °C, leaving 11.3% (by mass) inorganic solid. Apparently, the residual inorganic fraction is very low; however, the real proportion between ZrO_2 and the organic membrane is much higher considering the incomplete hydrolysis of the zirconium precursor under the present synthesis conditions. It was also found that the apparent residual inorganic fraction can be increased to more than 30% without changing the inner structure of the ZrO_2 material by increasing the concentration of the ZP solution and by repeated dipping and drying. The XRD patterns of the ESM/ZP hybrid as well as the ZrO_2 networks after calcination at 600 °C and 700 °C are shown in

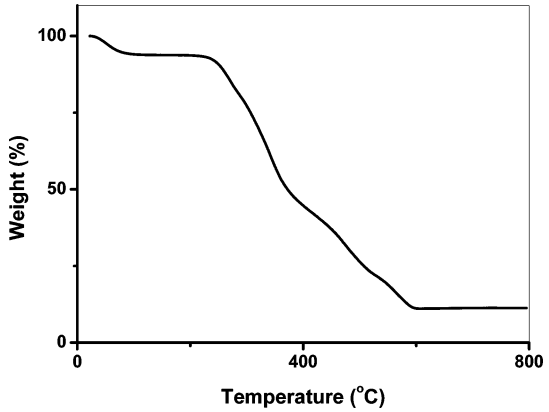

Fig. 2 TGA curve of as-synthesized ESM/ZP hybrid.

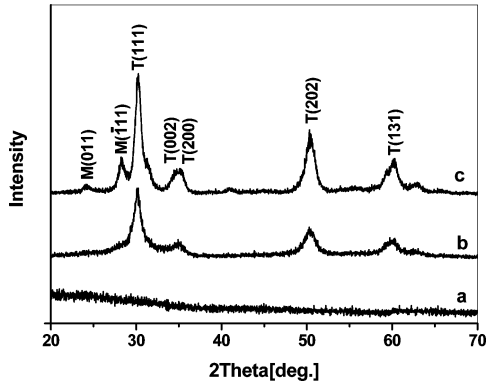

Fig. 3 XRD patterns of ESM-templated ZrO_2 samples: (a) as-synthesized ESM/ZP hybrid, (b) ZrO_2 networks obtained at 600 °C, (c) ZrO_2 networks obtained at 700 °C. T: tetragonal, M: monoclinic.

Fig. 3. It can be seen that the zirconium species involved in the ESM/ZP hybrid are totally amorphous. After calcination at 600 °C, the amorphous zirconium species crystallized into tetragonal zirconia accompanying the complete ESM pyrolysis. An average crystallite size of about 6 nm was estimated according to the line width analysis of the tetragonal ZrO_2 (111) diffraction peak based on the Scherrer formula. When the calcination temperature was increased to 700 °C, diffraction peaks corresponding to monoclinic ZrO_2 appeared in addition to those for tetragonal ZrO_2, which indicates that a tetragonal-to-monoclinic phase transformation occurred, leading to the formation of a mixture of tetragonal and monoclinic phases (Fig. 3c). It has been documented that precipitated amorphous ZrO_2 can crystallize into pure tetragonal ZrO_2, a metastable polymorph of zirconia, upon heat treatment and the tetragonal-to-monoclinic phase transformation may occur at various temperatures for nanocrystalline[29] or porous[34] ZrO_2 obtained under various conditions.

After the ESM/ZP hybrid was calcined at 600 °C, the membrane-like sample remained crack-free although it shrunk and crinkled significantly, and became rather fragile. A linear shrinkage to ~30% of the original membrane size upon calcination was observed. Typical SEM images of ESM-templated ZrO_2 networks obtained after calcination at 600 °C are shown in Fig. 4, which suggests that the overall network structure of the ESM template is fully retained although the networks have shrunk considerably. As shown in Fig. 4a, the obtained ZrO_2 networks are composed of interwoven and coalescing ZrO_2 fibers ranging from 0.3 to 1.0 μm in diameter, slightly smaller than the diameters of the membrane fibers (0.5–1.5 μm). On the other hand, the pore sizes of the apparent macropores are significantly decreased, indicating considerable shrinkage during template removal. Fig. 4b presents a SEM image of the cross section of the ZrO_2 networks, which shows that the product is actually a thin film with thickness around 15 μm. An enlarged image of the cross section (Fig. 4c) clearly shows that the ZrO_2 fibers constituting the networks are actually hollow tubes with a wall thickness less than 200 nm. Accordingly, it can be concluded that the obtained ZrO_2 material is hierarchically ordered macroporous networks consisting of hollow ZrO_2 tubes.

The hollow nature of the ZrO_2 fibers constituting the networks was further evidenced by TEM investigations. Fig. 5a shows a ZrO_2 tube with a diameter of about 400 nm and a wall thickness of about 50 nm. The corresponding electron diffraction pattern exhibits clear rings related to tetragonal ZrO_2, indicating that the ZrO_2 tubes comprise ZrO_2 nanocrystallites. A typical HRTEM image of the tube walls (Fig. 5b) revealed the presence of many nanocrystals showing clear (111) lattice fringes for tetragonal ZrO_2, confirming that the ZrO_2 tubes consist of tetragonal ZrO_2 nanocrystals (4–8 nm), which

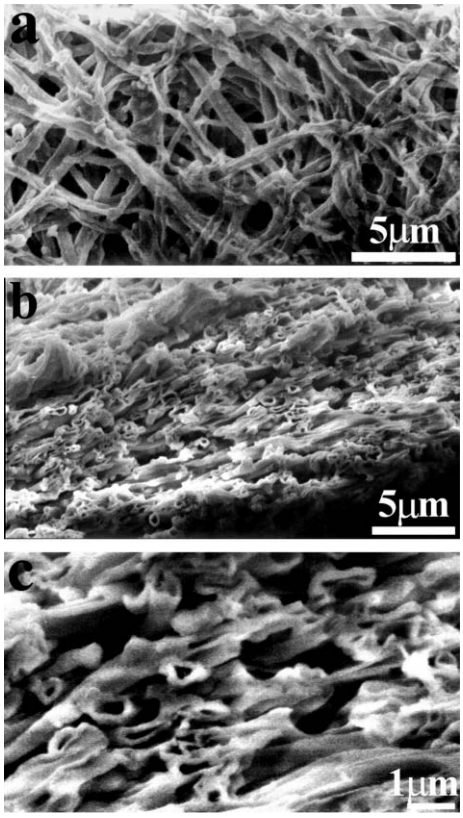

Fig. 4 SEM images of ESM-templated ZrO_2 networks obtained at 600 °C: a) overview of the surface, b) overview of the cross section, and c) higher magnification of the cross section showing the broken hollow tubes.

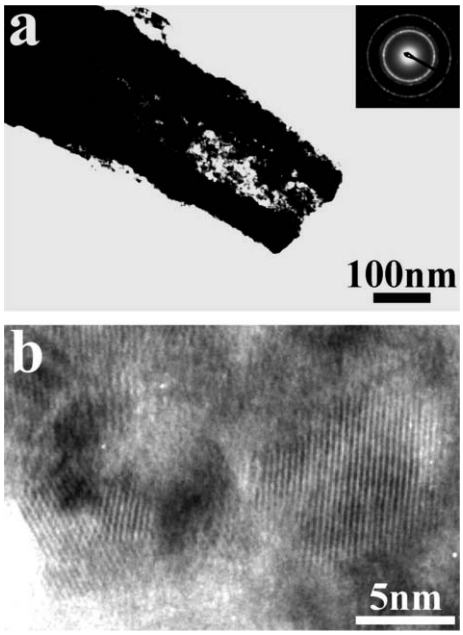

Fig. 5 TEM (a) and HRTEM (b) images of ZrO_2 tubes constituting the ZrO_2 networks obtained at 600 °C.

is consistent with the corresponding XRD result. It is noted that individual ZrO_2 tubes have been previously fabricated by templating carbon nanotubes[30] or alumina membranes;[31] however, to the best our knowledge, this is the first successful synthesis of hierarchically ordered macroporous networks composed of ZrO_2 tubes.

The nitrogen adsorption–desorption isotherms for the obtained ZrO_2 networks are presented in Fig. 6, which exhibit type IV isotherms with a hysteresis loop, indicating the

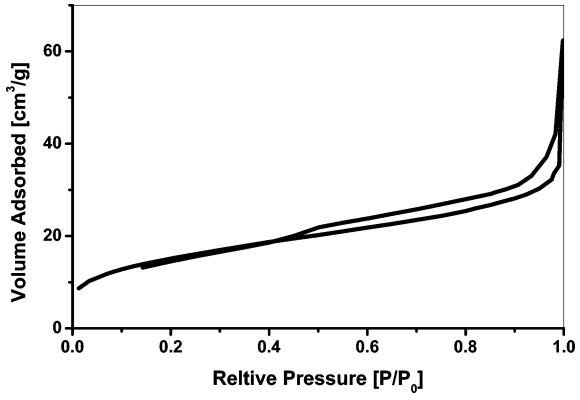

Fig. 6 Nitrogen adsorption–desorption isotherms of ESM-templated ZrO_2 networks obtained at 600 °C.

presence of mesopores. The Brunauer–Emmett–Teller (BET) surface area of the ZrO_2 networks was measured to be 55 m^2 g^{-1} and the BET average pore size was estimated to be 7.0 nm, confirming the presence of mesopores within the tube walls composed of ZrO_2 nanocrystals. The surface area value is considerably larger than that for the 3-D ordered macroporous ZrO_2 (monoclinic) obtained by colloidal crystal templating (38 m^2 g^{-1}),[35] and it is similar to that for the macroporous ZrO_2 networks obtained by sol–gel coating of CA membranes (54 m^2 g^{-1}) although it remains unclear whether this ZrO_2 material was crystallized.[12] The combination of high surface area and high porosity of macroporous crystalline ZrO_2 networks is expected to enhance the wide and ever-growing range of applications of zirconia. Moreover, the unique hierarchical characteristic of the current macroporous networks composed of ZrO_2 tubes comprising tetragonal ZrO_2 nanocrystals might endow this material with unusual properties of technological importance. These results demonstrate that the procedure of sol–gel mineralization of ESM can be readily extended to systems of metal oxides other than TiO_2, which represents a versatile method for the biomimetic synthesis of hierarchically ordered networks of metal oxides.

Calcination of the ESM/ZP hybrid at elevated temperatures resulted in significant fusion between neighboring ZrO_2 tubes accompanying the tetragonal-to-monoclinic phase transformation of zirconia. Fig. 7 illustrates typical SEM images of the ESM-templated ZrO_2 networks after calcination at 700 °C, which shows that the obtained porous networks are much denser than the networks obtained at 600 °C. Although the structure of a network consisting of hollow tubes is partly preserved near the surface of the membrane (Fig. 7a), the inner structure of the material looks more like a solid containing reticular hollow channels, the diameter of which is reminiscent of the diameter of the ESM fibers (Fig. 7b). This result is in good agreement with the general observations that the tetragonal-to-monoclinic phase transformation of zirconia is accompanied by volume expansion[29] and loss of porosity.[34] It is known that the tetragonal-to-monoclinic phase transformation of zirconia is of technological importance as it contributes to the toughening of ceramics.[29] Therefore, it is expected that the obtained macroporous crystalline ZrO_2 networks may find applications as a structural ceramic.

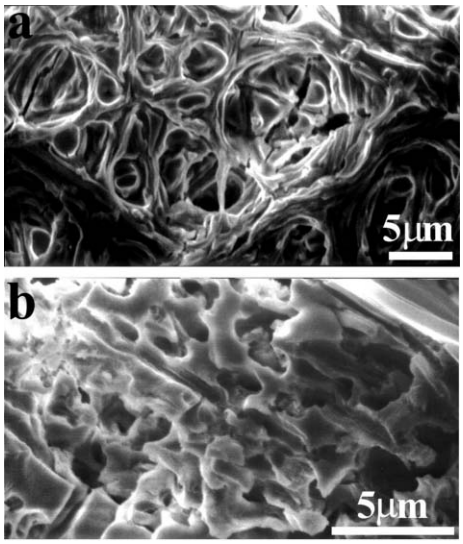

Fig. 7 SEM images of ESM-templated ZrO_2 networks obtained at 700 °C: a) the surface, and b) the cross section.

Conclusion

A facile sol–gel coating procedure has been successfully applied for the ZrO_2 coating of eggshell membranes (ESM), resulting in hierarchically ordered membranes with a structure of macroporous networks comprising crystalline ZrO_2 tubes. This hierarchical material, which has a specific surface area of 55 m^2 g^{-1} and a BET average pore size of 7.0 nm, was obtained through sol–gel mineralization of the ESM template and subsequent calcination at 600 °C. It shows a macroscopic morphology of a film with a thickness of about 15 μm; the film has a microstructure of macroporous networks composed of interwoven ZrO_2 microtubes with diameters less than 1.0 μm; the tube walls consist of tetragonal ZrO_2 nanocrystals with an average crystallite size about 6 nm. The combined benefits of macropores, microtubes, and mesopores can potentially be obtained in one film, which would make this material attractive for numerous applications including catalysis, separation, and sensors. It has also been revealed that calcination of the initial ESM/zirconium precursor hybrid at 700 °C resulted in a significant fusion between neighboring ZrO_2 tubes accompanying a tetragonal-to-monoclinic phase transformation of zirconia. These results suggest that the procedure of sol–gel mineralization of ESM represents a versatile method for the biomimetic synthesis of hierarchically ordered networks of metal oxides, which further demonstrates the great potential of bio-inspired materials chemistry.[40]

Acknowledgements

This work was supported by the National Natural Science Foundation of China (20003001, 20233010) and the Special Fund for Authors of Chinese Excellent Doctoral Theses, MOE, China (200020).

References

1 C. F. Blanford, H. Yan, R. C. Schroden, M. Al-Daous and A. Stein, *Adv. Mater.*, 2001, **13**, 401.
2 P. M. Tessier, O. D. Velev, A. T. Kalambur, A. M. Lenhoff, J. F. Rabolt and E. W. Kaler, *Adv. Mater.*, 2001, **13**, 396.
3 M. E. Turner, T. J. Trentler and V. L. Colvin, *Adv. Mater.*, 2001, **13**, 180.
4 S. Vaucher, E. Dujardin, B. Lebeau, S. R. Hall and S. Mann, *Chem. Mater.*, 2001, **13**, 4408.
5 Y.-J. Lee, J. S. Lee, Y. S. Park and K. B. Yoon, *Adv. Mater.*, 2001, **13**, 1259.
6 A. Imhof and D. J. Pine, *Nature*, 1997, **389**, 948.
7 J. Y. Ying, C. P. Mehnert and M. S. Wong, *Angew. Chem., Int. Ed.*, 1999, **38**, 56.
8 D. Y. Zhao, J. G. Feng, Q. S. Huo, N. Melosh, G. H. Fredrickson, B. F. Chmelka and G. D. Stucky, *Science*, 1998, **279**, 548; D. Y. Zhao, Q. S. Huo, J. G. Feng, B. F. Chmelka and G. D. Stucky, *J. Am. Chem. Soc.*, 1998, **120**, 6024.
9 P. Yang, D. Zhao, D. I. Margolese, B. F. Chmelka and G. D. Stucky, *Nature*, 1998, **396**, 152; P. Yang, D. Zhao, D. I. Margolese, B. F. Chmelka and G. D. Stucky, *Chem. Mater.*, 1999, **11**, 2813.

10 R. A. Caruso, M. Giersig, F. Willig and M. Antonietti, *Langmuir*, 1998, **14**, 6333; R. A. Caruso, M. Antonietti, M. Giersig, H.-P. Hentze and J. Jia, *Chem. Mater.*, 2001, **13**, 1114.
11 M. Breulmann, S. A. Davis, S. Mann, H.-P. Hentze and M. Antonietti, *Adv. Mater.*, 2000, **12**, 502.
12 R. A. Caruso and J. H. Schattka, *Adv. Mater.*, 2000, **12**, 1921.
13 R. A. Caruso and M. Antonietti, *Adv. Funct. Mater.*, 2002, **4**, 307.
14 D. Walsh, J. D. Hopwood and S. Mann, *Science*, 1994, **264**, 1576.
15 S. D. Sims, D. Walsh and S. Mann, *Adv. Mater.*, 1998, **10**, 151.
16 W. Ogasawara, W. Shenton, S. A. Davis and S. Mann, *Chem. Mater.*, 2000, **12**, 2835.
17 F. C. Meldrum and R. Seshadri, *Chem. Commun.*, 2000, 29; R. Seshadri and F. C. Meldrum, *Adv. Mater.*, 2000, **12**, 1149.
18 S. A. Davis, S. L. Burkett, N. H. Mendelson and S. Mann, *Nature*, 1997, **385**, 420.
19 B. Zhang, S. A. Davis, N. H. Mendelson and S. Mann, *Chem. Commun.*, 2000, 781.
20 Y. Shin, J. Liu, J. H. Chang, Z. Nie and G. J. Exarhos, *Adv. Mater.*, 2001, **13**, 728.
21 A. Dong, Y. Wang, Y. Tang, N. Ren, Y. Zhang, Y. Yue and Z. Gao, *Adv. Mater.*, 2002, **14**, 926.
22 D. Yang, L. Qi and J. Ma, *Adv. Mater.*, 2002, **14**, 1543.
23 S. Mann, *Angew. Chem., Int. Ed.*, 2000, **39**, 3392.
24 S. Mann, *Biomineralization. Principles and Concepts in Bioinorganic Materials Chemistry*, Oxford University Press, Oxford, 2001.
25 D. J. Suh and T.-J. Park, *Chem. Mater.*, 2002, **14**, 1452.
26 E. L. Crepaldi, G. J. de A. A. Soler-Illia, D. Grosso, P.-A. Albouy and C. Sanchez, *Chem. Commun.*, 2001, 1582.
27 M. Vallet-Regí, S. Nicolopoulos, J. Román, J. L. Martínez and J. M. González-Calbet, *J. Mater. Chem.*, 1997, **7**, 1017.
28 S. Benfer and E. Knözinger, *J. Mater. Chem.*, 1999, **9**, 1203.
29 S. Shukla, S. Seal, R. Vij, S. Bandyopadhyay and Z. Rahman, *Nano Lett.*, 2002, **2**, 989.
30 C. N. R. Rao, B. C. Satishkumar and A. Govindaraj, *Chem. Commun.*, 1997, 1581.
31 J. Bao, D. Xu, Q. Zhou, Z. Xu, Y. Feng and Y. Zhou, *Chem. Mater.*, 2002, **14**, 4709.
32 D. Khushalani, G. A. Ozin and A. Kuperman, *J. Mater. Chem.*, 1999, **9**, 1491.
33 E. Zhao, O. Henrández, G. Pacheco, S. Hardcastle and J. J. Fripiat, *J. Mater. Chem.*, 1998, **8**, 1635.
34 G. Pacheco and J. J. Fripiat, *J. Phys. Chem. B*, 2000, **104**, 11906.
35 B. T. Holland, C. F. Blanford and A. Stein, *Science*, 1998, **281**, 538.
36 R. A. Caruso and M. Antonietti, *Chem. Mater.*, 2001, **13**, 3272.
37 M. T. Hincke, J. Gautron, M. Panheleux, J. Garcia-Ruiz, M. D. McKee and Y. Nys, *Matrix Biol.*, 2000, **19**, 443.
38 J. E. Dennis, D. A. Carrino, K. Yamashita and A. I. Caplan, *Matrix Biol.*, 2000, **19**, 683.
39 S. Ishikawa, K. Suyama, K. Arihara and M. Itoh, *Bioresour. Technol.*, 2002, **81**, 201.
40 E. Dujardin and S. Mann, *Adv. Mater.*, 2002, **14**, 775.